

## Low-Cost GNSS Interferometric Reflectometry (GNSS-IR) Sensor for Potential Long-Term Coastal Sea Level Monitoring

Dave Liam T. Ngo<sup>2</sup>, John Michael Rey A. Zamora<sup>2,4</sup>, Rosalie B. Reyes<sup>1,2</sup>, Leila Micahella D. Cruz<sup>2,3</sup>, Jasper D. Molleno<sup>2</sup>, John Dave C. Maclang<sup>2</sup>, Alexi Mae Y. Narca<sup>2</sup>, Luis Carlos S. Mabaquiao<sup>1,2</sup>, Hanna Mae M. Garcia<sup>1,2</sup>, Dennis Arsenio B. Bringas<sup>5</sup>, Shelmark S. Peñaranda<sup>5</sup>, Beaverlex N. Algaba<sup>5</sup>, Arvin Joshua P. Venerable<sup>5</sup>

<sup>1</sup> Department of Geodetic Engineering, University of the Philippines, Diliman, Quezon City, Philippines - rbreyes3@up.edu.ph, {lsmabaquiao, hhgarcia1}@up.edu.ph

<sup>2</sup> Training Center for Applied Geodesy and Photogrammetry, University of the Philippines, Diliman, Quezon City, Philippines - {dtng01, jazamora2, ldcruz6, jbmolleno, jcmaclang, aynarca}@up.edu.ph

<sup>3</sup> Marine Science Institute, University of the Philippines, Diliman, Quezon City, Philippines

<sup>4</sup> Electrical and Electronics Engineering Institute, University of the Philippines, Diliman, Quezon City, Philippines

<sup>5</sup> Physical Oceanography Division, Hydrography Branch, National Mapping and Resource Information Authority, Manila, Philippines - {dabringas, sspenaranda, bnalgaba, ajpvenerable}@namria.gov.ph

**Keywords:** GNSS, GNSS Interferometric Reflectometry, Sea Level Monitoring, Signal-to-noise Ratio (SNR), Raspberry Pi

### Abstract

In the continued exploration of Global Navigation Satellite System (GNSS) technologies, remote sensing using interferometric reflectometry (IR) has emerged as a promising method for surface monitoring through the analysis of multipath signals. Due to this unique method of capitalizing an error source of GNSS signal to determine environmental parameters, this research aims to monitor coastal sea level by developing and assembling a low-cost GNSS-IR sensor system, and to compare its measurements with data from a traditional tide gauge. A u-blox F9P receiver in tandem with a u-blox ANN-MB-00 antenna oriented towards the first Fresnel Zone (FFZ) for optimal retrievals was connected to a solar-powered Raspberry Pi single-board computer. Remote device monitoring and GNSS data logging were done using an open-source web server hosted through PiTunnel. The acquired data was then processed through *gnssrefl*, employing advanced outlier removal, bias corrections, and height adjustments, thus accurately capturing sea level trends. The deployed station in Limay, Bataan, showcased continuous operation over a course of 15 days with minimum physical intervention and technical issues encountered. Meanwhile, the GNSS-IR measurements show strong alignment with the tide gauge record, with an RMSE of 3.115 cm, MAE of 2.240 cm, and a Pearson correlation of 0.997, indicating excellent performance in capturing sea level variations. From these results, it can be inferred that the GNSS-IR technique demonstrated through a low-cost and reliable sensor system is a viable alternative for long-term coastal sea level monitoring.

### 1. Introduction

#### 1.1 Background of the Study

As the global climate continues to experience consistent temperature rise, one of the effects of the rapidly changing environment is the rising sea level. Particularly in the Philippines, the mean rate of sea level rise is not only faster than the global average, but the country's archipelagic nature renders it more sensitive to sea level rise (Siringan and Sta. Maria, 2024). Thus, long-term and large-scale monitoring of coastal sea levels has become a necessity. While sensors such as traditional tide gauges (TGs) have been reliably used for these purposes, disadvantages like susceptibility to vertical land movement, vulnerability to water corrosion, frequent maintenance, and overall larger costs have somewhat limited its scope and application. However, an emerging technique for environmental monitoring, particularly sea level altimetry, by exploiting the Signal-to-Noise Ratio (SNR) data of both the direct and reflected GNSS signals has come to light in the form of GNSS interferometric reflectometry (GNSS-IR).

Paired with advancements in microelectronics and Internet-of-Things (IOT) technology, this method not only provides a cost-effective alternative to traditional TGS by utilizing commercial-off-the-shelf (COTS) GNSS receivers and single-board computers (SBCs), but it can also supplement its results while remaining unaffected by factors such as land subsidence and crustal movements (Larson et al., 2013).

Moreover, its potential for reliable long-term operation and real-time monitoring is essential not only for analyzing the effects of rising sea levels but also for providing valuable insights to decision-makers and policymakers in risk mitigation, especially for coastal communities.

#### 1.2 Research Objectives

This study aims to demonstrate a GNSS-IR system for measuring coastal sea level using commercially available components. In doing so, the research holds the following specific objectives:

1. Design, develop, and deploy a sensor station integrating off-grid power supply, GNSS data acquisition, and remote monitoring;
2. Measure SNR data and calculate the corresponding reflector height and sea level;
3. Validate and compare results with a co-located geodetic-quality tide gauge;
4. Assess the sensor system's performance for long-term monitoring.

### 2. Related Literature

#### 2.1 GNSS-IR Concepts and Principles

GNSS is a well-established technology that is used extensively in Position, Navigation, and Timing (PNT). Continued research

efforts in the last three decades on analyzing error sources such as multipath in conventional GNSS signals have shown promising results for ocean and land remote sensing use. This paved the way for GNSS reflectometry (GNSS-R), which demonstrated that the properties of signals change as it is reflected from a surface. Then, the reflecting surface's properties can be inferred based on these changes (Xu et al., 2024). GNSS-R is mainly used in airborne and spaceborne instrumentation, where the time delay between direct and reflected signals is used to calculate the sea level. Meanwhile, GNSS-IR is focused on ground-based measurements of multipath signals and their constructive/destructive interference that can be observed through the SNR data, in which the corresponding reflector height and sea level can be calculated (Larson and Williams, 2023). Figure 1 shows a diagram of the geometry of expected direct and multipath signals in GNSS-IR.

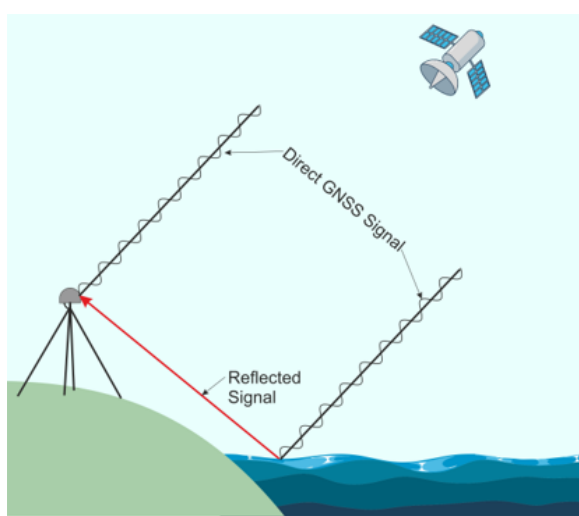


Figure 1. GNSS-IR reflection geometry (Permanent Service for Mean Sea Level, n.d.).

Aside from water level monitoring, extracted SNR data can also provide insight into properties of the antenna's surroundings, such as vegetation height, soil moisture, or snow depth and accumulation (Abdelhamid and Maciuk, 2025). Of these applications, the ability to measure and monitor coastal sea levels is particularly appealing here in the Philippines, as an archipelagic country that is vulnerable to the impacts of climate change and rising mean sea level.

Another property of GNSS-IR observations that must be considered is the Fresnel zones of the location in which the receiver antenna is set up. Fresnel zones are concentric ellipsoidal regions that surround the direct line-of-sight path between a GNSS satellite and the receiver. These zones are defined based on the elevation and azimuth angles of the satellite and the distance to the reflecting surface. The FFZ is particularly significant in GNSS-IR applications, as it determines the area from which reflected signals can constructively interfere with the direct signal, enhancing the SNR (Larson and Williams, 2023). In the context of sea level monitoring, understanding the Fresnel zones is essential for optimizing data accuracy and sensor placement. The size and shape of these zones influence the spatial resolution and accuracy of measurements related to sea surface height. Researchers can extract valuable data on sea level variations by analyzing the interference patterns within these zones (Roesler and Larson, 2018; Larson and Williams, 2023).

## 2.2 GNSS-IR for Sea Level Monitoring

One of the early demonstrations of GNSS-IR for water level monitoring used a geodetic-grade GNSS antenna to measure the water level of Kachemak Bay, Alaska, over one year. This resulted in a daily average of 2.3 cm agreement with a traditional tide gauge, thus providing evidence of the technology's ability for this application. (Larson et al., 2013).

Additionally, a geodetic-quality GPS tide gauge in Onsala, Sweden, with zenith-pointing and nadir-pointing antennas also demonstrated GNSS-IR capability for coastal sea level measurements with precision of <5 cm (Larson et al., 2013). In a similar study, a GNSS-IR station was used to monitor the water level of Lake Taupo in New Zealand over the course of 10 years. While focusing on a different type of body of water as this study, the core instrumentation and data processing of GNSS-IR remains. The findings showed that water levels determined were found to be within  $\pm 0.069$  m and  $\pm 0.124$  m of water levels determined by radar altimetry (Holden and Larson, 2021). Furthermore, it is also worth noting that the deployed station was continuously running for 10 years using an off-grid solar power supply. This demonstrated high potential for the utilization of GNSS-IR stations as permanent installations for monitoring purposes.

## 2.2 Low-Cost System for GNSS Data Acquisition

Widespread adoption of the GNSS-IR technique as a viable alternative to traditional TGs requires it to be integrated in a system that is relatively cheap, readily available, easily assembled, and needs less maintenance. Consequently, GNSS deployments are typically partnered with computer systems (Baklan, 2012) used to record satellite observations made by the GNSS receivers. This requirement often bars static systems from being deployed in remote settings wherein power may be limited and calls for a need for human intervention to manage as well as connection to power grid to act as a continuous and reliable observing station.

However, given recent technological advancements in embedded systems, data communications, and access to open-source software and hardware designs, low-cost GNSS-IR sensors using COTS components have seen a prominent rise in utilization. The system was able to yield stable measurements with an RMSE of 16 cm using an Android smartphone and a low-cost antenna connected to a GNSS receiver (Chen et al., 2023). Also, an Arduino-based GNSS-IR sensor was deployed and evaluated for almost one year, which yielded an RMSE of 2.9 cm (Fagundes et al., 2021). Meanwhile, a cost-efficient multi-GNSS prototype assembly for geodynamics application employed a Raspberry Pi-based sensor module (Vidal et al., 2024). Whereas, for water level monitoring, a Raspberry Pi reflector was developed with centimeter-level accuracy and operated for nearly two years without requiring any on-site calibration. (Karegar et al., 2022).

## 3. Instrumentation

### 3.1 Hardware and Electronics

A low-cost GNSS-IR sensor station was developed and installed at Lamao Port in Limay, Bataan, to monitor the nearby coastal sea level and assess its performance for possible long-term operation and application in other areas.

The system consists mainly of the following components:

- u-blox ANN-MB-00 GNSS Antenna
- u-blox F9P GNSS Receiver
- Raspberry Pi 4B
- 4G USB WiFi Modem and Sim Card
- 12V 20A Solar Charge Controller
- 12V 100Ah LiFePO4 Battery
- 100W Solar Panel

The GNSS-IR station acts similarly to a Continuously Operating Reference Station (CORS) albeit with key differences integral to its IR capabilities. Firstly, as a sea level monitoring instrument, the station must be installed in close proximity to the subject body of water – this being said, the system must reliably operate off-grid as power sockets are typically unavailable in this setting. Secondly, the receiver and antenna also work against conventional practices, often disregarding the use of a ground plane, disabling certain filtering protocols such as its elevation mask, and in certain applications, may use the antenna on its side rather than pointing up.

The sensor assembly can be categorized into two parts: power generation and data collection. The data collection components involve the reception and storage of GNSS data – specifically, the Raspberry Pi, u-blox receiver and antenna. Meanwhile, a 4G USB WiFi Modem with an active mobile data subscription was used to provide internet connectivity for remote data transmission. Likewise, the station is powered by an off-grid photovoltaic (PV) system using a 100 W solar panel, 1200 Wh LiFePO4 battery, and a 20A charge controller to prevent overcharging and damage to both the panel and battery. The system's functional blocks and their corresponding interconnections are as follows:

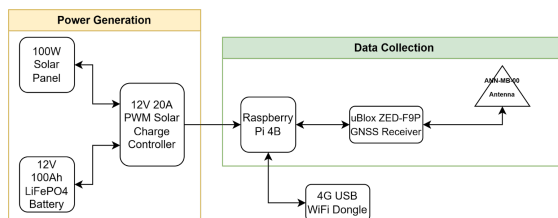


Figure 2. System Block Diagram of the Deployed GNSS-IR Station.

All components were connected through appropriate electrical wires and adapters, then secured inside a weatherproof enclosure and railings. Furthermore, the enclosure was modified to allow wires to be securely passed through using electrical glands, and additional ventilation holes were drilled into the bottom of the enclosure to provide additional airflow and cooling.

The GNSS antenna was then routed through a gland into the housing and is mounted on an external pole near a TG. The configured antenna orientation and height that are crucial for proper data acquisition were selected based on the Fresnel zone surrounding the antenna. This will be further discussed in the next section.

In terms of power consumption, the system aims to operate continuously after deployment and requires 437.4 Wh daily without losses. Given the location, the PV system used is expected to provide the power needed for the station.

In total, the summarized bill of materials for the system is tabulated in Table 1 below:

Item	Price
U-blox F9P Receiver	PHP 13,203
U-blox ANN-MB-00 Antenna	PHP 3,341
Raspberry Pi 4B	PHP 7,689
100W Solar Panel	PHP 2,000
PWM Solar Charge Controller	PHP 616
12V LiFePO4 Battery	PHP 8,400
USB WiFi Modem and Sim Card	PHP 400
Housing	PHP 4,193
Misc. wires and connectors	PHP 1,000
<b>Total</b>	<b>PHP 40,842</b>

Table 1. Summarized Cost of Materials for GNSS-IR System

The assembly and connection of the components within the housing are shown as a whole in figure 3:



Figure 3. Internal System Assembly.

Likewise, a closer view of the data collection assembly is shown in figure 4:



Figure 4. Data Collection Block Assembly.

### 3.2 Data Acquisition and Remote Monitoring Tools

In conventional GNSS station setups, data retrieval is often performed through direct onsite access, such as manually acquiring logged data via external storage devices. While effective, this method is labor-intensive, prone to delays, and less practical for stations deployed in remote or coastal locations. To address these limitations, this study instead explores and implements remote access solutions for both data acquisition and system monitoring, thereby enabling continuous, efficient, and secure operation without requiring frequent physical intervention.

To allow remote device monitoring and data retrieval, the Raspberry Pi was also equipped with the following programs:

- RTKBase
- PiTunnel
- Raspberry Pi Connect

RTKBase is an open-source web server software that provides multiple functions essential to GNSS-IR applications like GNSS receiver configuration, data logging and log files management, file conversion, and data downloading capability. Consequently, the device information, like CPU temperature, uptime, and disk storage, is also updated in the dashboard in real-time (Stefal, 2025). The software is typically used for base stations in positioning applications; while the study's application of the software is a slight departure from its intended purpose, its data logging and management can still be utilized. Figure 5 showcases this dashboard from which signal status, settings, and logs are accessed.



Figure 5. RTKBase GNSS Signal Status Dashboard.

Due to the application being accessible only through a local area connection, a tunneling service such as PiTunnel was necessary for hosting an HTTP web server like RTKBase, allowing said dashboard to be accessed through any device with an internet connection. The software, as presented in figure 6 also comes with the benefit of being able to track in real-time the status of different parameters of the host device, as well as email alerts to the user for status such as device online/offline, memory, disk, CPU usage, and CPU temperature.

Finally, the installation of Raspberry Pi Connect serves as a means of full remote access to the Raspberry Pi unit, and provides redundant monitoring and serves as an additional platform for diagnosis and troubleshooting.

Altogether, these services provide a remotely accessible station with redundancy checks that provide ample data for troubleshooting and diagnosis of possible errors encountered.

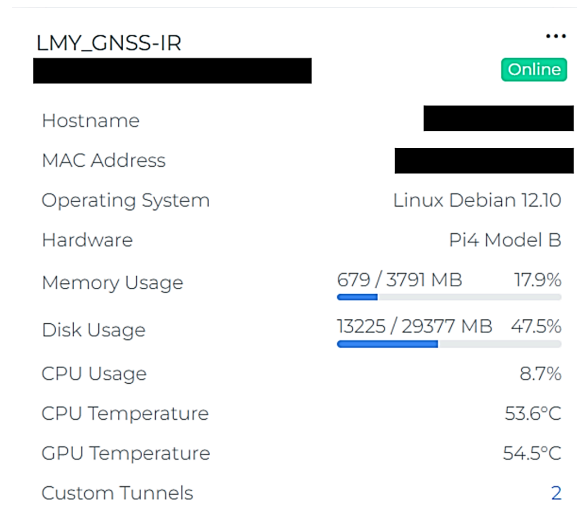


Figure 6. PiTunnel GUI Summarizing Host Status.

## 4. Methodology

### 4.1 Sensor Deployment and Data Acquisition

An initial assembly and testing of the sensor station were conducted in the University of the Philippines' premises to verify its functionality and perform minor adjustments in preparation for the actual on-site deployment. Prior to data acquisition, proper assembly and installation of the sensor are necessary. This was done by ensuring the following criteria:

1. Suitable area selection
2. Compatible Fresnel zone orientation
3. Proper antenna orientation

#### 4.1.1 Suitable Area Selection

Like traditional GNSS applications, a suitable area is important as this dictates the system's ability to receive satellite signals. This being the case, GNSS-IR setups require an open area and a clear view of the sky. Furthermore, the position of said sensor must also be within direct line-of-sight with the subject surface, which in the cases of sea level monitoring, typically leads to the station being positioned along the coast or integrated in facilities that extend into the bodies of water, such as ports or monitoring facilities. In either case, the sensor must capture the subject surface within the Fresnel zone.

In line with needing the subject surface to be within the Fresnel zone, the antenna's height also plays a great importance as a higher antenna position also provides a larger Fresnel zone. While this allows for more coverage of the subject surface, in some cases, this may also lead to the introduction of other surfaces being captured in the reflected signals, thus complicating data processing.

#### 4.1.2 Compatible Fresnel Zone Orientation

Another property of Fresnel zones that must be considered is a "blind spot" caused by satellite orbital geometry. The specific location of this blind spot varies with latitude, but it typically appears in the northern portion of the Fresnel zone in the Philippines, which lies in the Northern Hemisphere (Larson, 2024). Figure 7 displays an example of this, with the full Fresnel zone of the proposed antenna located in Limay, Bataan. Note that even in the full Fresnel zone, a segment of the zone is absent on the northern side. Because of this property, it would be ill-advised to position the antenna facing this side.



Figure 7. Default Fresnel Zone Map (Left) and Masked (Right).

Looking at the fresnel zone comparison in Figure 7, the full Fresnel zone also consists of sections of land. As only water is needed, only the Fresnel zones from azimuths 0 to 240° from the North were considered. This effectively masks out other

surfaces and leaves only the desired subject surface. Given the natural blind spot of Fresnel zones, it is ideal for sea level monitoring if the land occupies this blind spot. This configuration allows the reflective surface, the sea to the south, to coincide with the more sensitive portions of the Fresnel zone, therefore maximizing the quality of GNSS-IR for sea level measurements.

#### 4.1.3 Proper Antenna Orientation

From the identified fresnel zone, the masked area of interest is towards the southeastern side. Unlike typical positioning applications, the antenna is not positioned upright, but rather on its side in order to receive more reflected signals. The antenna was oriented to face said southeastern side of the port as opposed to the traditional method of having an antenna pointing towards the sky to maximize the retrievals. In other words, the antenna must point to the body of water, towards where most of the Fresnel zone lies. The installation of the antenna is illustrated in Figure 8. Here, an antenna height of 3.5 m was adopted.



Figure 8. Antenna Oriented Towards the Water Surface.

#### 4.2 Signal-to-Noise Data Processing

The reflector height is computed by identifying the dominant oscillation frequency  $f$  in the detrended SNR vs  $\sin e$  in the Lomb-Scargle periodograms (LSP). Within this framework, reflector heights are directly computed using the following formula (1) (Larson et al., 2013)

$$H = \frac{f\lambda}{2 \sin e} \quad (1)$$

where  $H$  = reflector height  
 $f$  = dominant oscillation frequency  
 $\lambda$  = wavelength of the GNSS signal  
 $e$  = satellite elevation angle

Moreover, Larson et al. (2013) proposed a correction since the derivation of the formula (2) assumes that the reflecting surface is static, whereas in reality, the water surface is time varying. Larson et al. (2013) showed that the height of the water level is changing at a rate of  $\dot{h}$  and the satellite elevation angle at a rate of  $\dot{e}$ , then the true instantaneous water level should be corrected by subtracting the term:

$$h_{corr} = \frac{\dot{h}}{\dot{e} \tan e} \quad (2)$$

where  $h_{corr}$  = height rate correction

$\dot{h}$  = height rate of change

$\dot{e}$  = satellite elevation rate of change

$e$  = satellite elevation

These computations and other corrections, such as atmospheric and tropospheric delay corrections, are embedded in the *gnssrefl* software used in the study.

### 5. Results and Discussion

In evaluating the acquired data and the results of the transpired deployment, notable observations in terms of the sensor itself, the observed data, and the accuracy against the sea level determined from a traditional tide gauge are hereby presented.

#### 5.1 System Assembly and Performance

First, the use of a u-blox F9P receiver was chosen due to its ability to log RAWX and SFRBX data, which are essential to convert the logged files from the proprietary UBX file extension to the RINEX file format for data processing. While these capabilities are not exclusive to the F9P, this receiver was selected due to its reliability and availability.

Next, the utilization of a USB WiFi Module was necessary as it is automatically active so long as it receives power and has an active mobile data load; thus, minimizing the need for human intervention as opposed to typical pocket WiFi modems that are manually turned on. Likewise, the selection of a Raspberry Pi unit benefits from this same property alongside being a cost-effective way to collect and manage data. Its small form factor, ease of integration and connectivity via USB ports and WiFi, remote access capability via secure shell (SSH) and VNC screen sharing, and its scalability for future sensor integration while consuming relatively low power proves it to be a good microcomputer option, especially for long-term operation.

Data management and acquisition conducted through RTKBase have also proven to be streamlined. The web server not only provides real-time device status but also access to the collected data at 24-hour rollover periods. These files were all readily accessible for download and file conversion through the user interface, alongside 60 days of past observation files as shown in figure 9.

File name	SETTINGS		actions
	type	size (MB)	
2025-06-04_00-00-00_GNSS-1.ubx.tag	TAG	0.85	
2025-06-04_00-00-00_GNSS-1.ubx	UBX	77.57	
2025-06-03_06.zip	ZIP	217.83	
2025-06-03_00-00-00_GNSS-1.ubx.tag	TAG	4.97	
2025-06-03_00-00-00_GNSS-1.ubx	UBX	460.31	
2025-06-02_06.zip	ZIP	217.56	
2025-06-01_06.zip	ZIP	211.83	
2025-05-31_06.zip	ZIP	209.85	
2025-05-30_06.zip	ZIP	211.47	
2025-05-29_06.zip	ZIP	218.22	
2025-05-28_06.zip	ZIP	217.34	
2025-05-27_06.zip	ZIP	222.15	

Figure 9. RTKBase GNSS Data Logs Interface.

Over the course of the observation period, the system experienced no downtime as shown in the device uptime data

in Figure 10, with the only period of inaccessibility occurring after a fluctuation in cellular signal was experienced in the area. As the data gathering was not reliant on an internet connection, the sensor was still able to collect data continuously.

Gnss receiver:	U-blox_ZED-F9P - 1.32
Board:	Raspberry Pi 4 Model B Rev 1.2
Os:	Debian 12 (Bookworm)
CPU Temp:	51.6 C° - (highest record: 62.8C°)
Uptime:	18d 34mn 46s
Storage:	15.81GB available of 30.8GB - (45.9 % used)

Figure 10. RTKBase System Status Interface.

## 5.2 Sea Level for Observation Period

After computation of reflector heights, 81 outliers are filtered using a standard deviation and excluded values exceeding 2.5 times the standard deviation from the daily average. Values under 4.5m, as seen from Figure 11, usually correspond to non-water surface (i.e., ground, vegetation, or docking boats) and are discarded during this filtration process. In practice, this threshold removes anomalously low measurements relative to the local mean and daily variability; these values occur when reflections come closer than the true water surface and might bias the sea level upward. Below, the points colored red indicate outliers which were removed from the set of reflector heights making use of the daily average in blue.

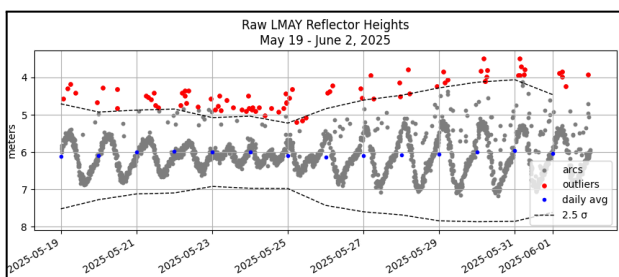


Figure 11. Raw Reflector Heights Filtered using Standard Deviation.

Once the gross outliers were removed, height corrections and interferometric bias correction were applied. Following those corrections, a second filtration using  $3\sigma$  was performed on the corrected reflector heights. The tighter  $3\sigma$  threshold further eliminates any remaining points that deviate strongly from the post-bias-corrected distribution, improving the precision of each reflector height observation. The result of these steps is a time series that can be interpreted as true sea level height at Limay Port, as shown in Figure 12.

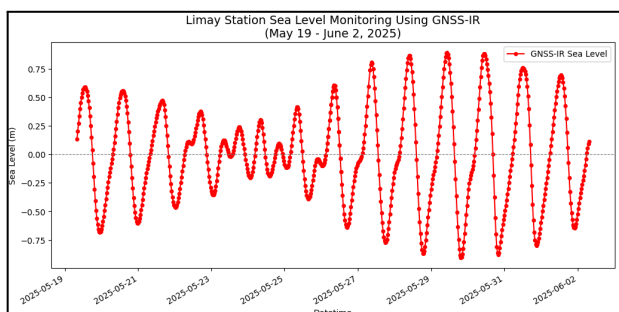


Figure 12. GNSS-IR Sea Level from May 19 to June 2.

The filtered and corrected reflector height shows a tidal-like oscillatory pattern over time, consistent with Cahyadi et al. (2023), who observed similar harmonic behavior in GNSS-IR measurements near river mouths influenced by sea tides.

## 5.3 Data Validation Against Tide Gauge

The filtered GNSS-IR measurements were compared against the co-located NAMRIA tide gauge. As seen in Figure 13, the GNSS-IR closely matches the validation tide gauge data trend with the GNSS-IR sea level indicated with red points while the sea level from the NAMRIA tide gauge is illustrated in blue.

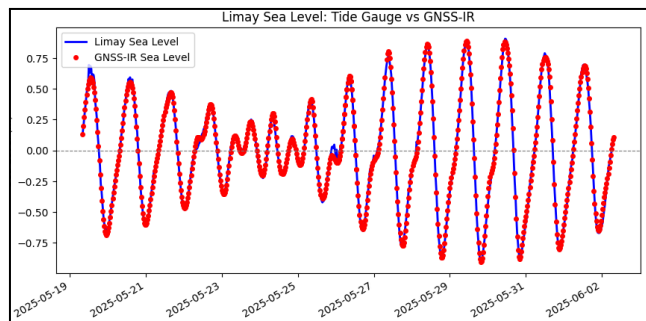


Figure 13. Comparison of Sea Level Heights of GNSS-IR and NAMRIA Co-located Tide Gauge.

The GNSS-IR time series agrees closely with the co-located NAMRIA tide-gauge record. An RMSE of 3.115 cm and an MAE of 2.230 cm indicate only minor discrepancies between the two sensors, while the Pearson correlation coefficient of 0.997 confirms an almost perfect linear association. The tight clustering of points about the 1:1 reference line in Figure 14 further emphasizes the consistency of the two data sets across the entire observation period.

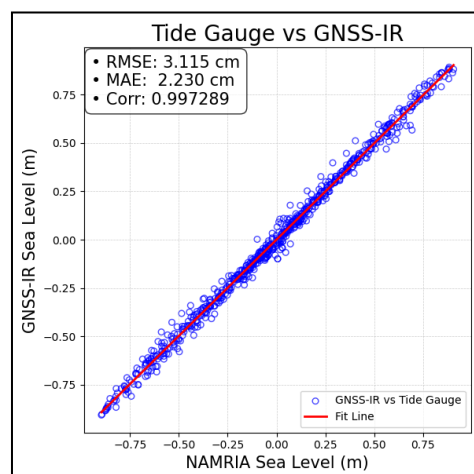


Figure 14. Regression Analysis of GNSS-IR and Tide Gauge.

## 6. Conclusions and Recommendations

### 6.1 Conclusions

A Raspberry Pi-based GNSS-IR sensor station was developed and deployed using a commercially available GNSS receiver and antenna to monitor the coastal sea level at Limay, Bataan. The station was powered by an off-grid PV system and integrated with a WiFi module to enable internet connectivity and remote access. GNSS data acquisition and system monitoring were managed through RTKBase, an HTTP web

server application routed via a custom tunneling service to ensure secure and continuous remote access. Compared to conventional TG systems, the proposed station provides a cost-effective and low-maintenance solution optimized for long-term coastal monitoring.

Throughout the observation period from May 19 to June 2, 2025, the system operated continuously without downtime, successfully generating daily UBX files for GNSS data processing. Hardware performance remained stable, with the recorded CPU maximum temperature of 62.8 °C, well below the Raspberry Pi's maximum temperature specification of 85 °C, demonstrating the resilience of the system to environmental conditions. These results highlight the capability of the station for potential long-term autonomous monitoring and its potential scalability beyond sea level measurements to other geodetic and remote sensing applications.

Meanwhile, the GNSS-IR technique employed in the station successfully retrieved sea level estimates at Limay Port for the observation period. Through a combination of statistical outlier filtering, height and bias corrections, and refined post-processing using a  $3\sigma$  threshold, a reliable time series of sea level heights was obtained. The resulting GNSS-IR measurements display a consistent tidal pattern and exhibit strong agreement with the co-located tide gauge. With an RMSE of 3.115 cm, MAE of 2.230 cm, and a Pearson correlation coefficient of 0.997, the GNSS-IR approach demonstrates high accuracy and precision, confirming its suitability as a complementary method for sea level monitoring at this site.

## 6.2 Recommendations

Based on the results of this study, it is recommended that the GNSS-IR sensor station be deployed for extended coastal sea level monitoring, with routine system diagnostics to ensure hardware stability and mitigate potential downtimes, particularly in remote areas where environmental factors may compromise system reliability. Additional receiver stations for areas with a nearby TG should also be considered for further validation and expansion of coastal sea level monitoring operations. In other settings however, installments must consider local factors such as site geography and solar irradiance. Particularly with the latter, adjustments to the power block may be necessary in areas with poor irradiance.

Further studies may also look into alternative receivers, software, or codes that allow for data logging as the *gnssrefl* software takes advantage of the open format RINEX in its processing keeping it from being locked behind proprietary formats.

To advance applications such as coastal hazard assessment and operational tide forecasting, future research should prioritize the development of near real-time GNSS-IR tide height monitoring systems. The integration of advanced Kalman filtering techniques, such as the Unscented Kalman Filter, can enable continuous and accurate reflector height estimation from dynamic and noisy SNR data streams (Strandberg et al., 2019). These approaches enhance both measurement precision and temporal resolution under varying satellite visibility and signal conditions, positioning GNSS-IR as a viable alternative or complement to conventional tide gauge networks, especially in data-sparse or remote coastal regions.

It is further recommended to adopt a dynamic operational framework, incorporating dynamic Fresnel zone calibration that adjusts for variations in satellite elevation angles and integrates tidal constituents to account for periodic changes in sea surface height, improving the accuracy of reflection geometry estimation. Long-term performance assessment, with a minimum observation period of at least one year, is recommended to evaluate system stability across seasonal variations. To further ensure continuous operation, especially during periods of limited solar irradiance, the integration of hybrid solar-wind power systems should be considered.

The implementation of real-time data processing algorithms may facilitate immediate SNR analysis and near-instantaneous sea level estimation, enhancing the capability of the system for autonomous and continuous monitoring. Finally, remote monitoring of multiple GNSS-IR receiver stations deployed across several sites must be integrated and streamlined where each station status and sea-level data will be displayed through a dashboard.

## Acknowledgements

We would like to acknowledge the following entities for their support throughout the implementation of this study. To DOST-PCIEERD, for their funding of the GNSS-IR project for sea level determination – we value the faith you have put in our capabilities to deliver on this study; Dr. Kristine Larson and Dr. Makan Karegar whose insights contribute greatly to the discipline, and to the GNSS-IR community; NAMRIA, for their continued aid and support in our fieldworks and data requests; Jacqueline Baluyot, Jake Nerval, and Arjay Cruz for providing integral support to the project and its researchers; The Filipino People, whom we continue to serve; and the Lord God for the continued blessings this project has received.

## References

Abdelhamid, M., Maciuk, K., 2025: The applications of GNSS-IR (Global Navigation Satellite System Interferometric Reflectometry): a comprehensive review. *Advances in Space Research*. doi.org/10.1016/j.asr.2025.05.080

Bakuła, M., 2012. An approach to reliable rapid static GNSS surveying. *Survey Review*, 44(327), 265–271. doi.org/10.1179/1752270611y.0000000038

Cahyadi, M.N., Bawasir, A., Susilo, Arief, S., 2023: Analysis of water level monitoring using GNSS interferometric reflectometry in river waters. IOP Conf. Ser.: Earth Environ. Sci., 1276(1), 012020. doi.org/10.1088/1755-1315/1276/1/012020.

Chen, L., Chai, H., Zheng, N., Wang, M., & Xiang, M., 2023. Feasibility and performance evaluation of low-cost GNSS devices for sea level measurement based on GNSS-IR. *Advances in Space Research*, 72(11), 4651–4662. doi.org/10.1016/j.asr.2023.07.031

Fagundes, M. A. R., Mendonça-Tinti, I., Iescheck, A. L., Akos, D. M., & Geremia-Nievinski, F., 2021. An open-source low-cost sensor for SNR-based GNSS reflectometry: design and long-term validation towards sea-level altimetry. *GPS Solutions*, 25(2). doi.org/10.1007/s10291-021-01087-1

Holden, L. D., & Larson, K. M., 2021. Ten years of Lake Taupō surface height estimates using the GNSS interferometric

reflectometry. *Journal of Geodesy*, 95(7).  
doi.org/10.1007/s00190-021-01523-7

Karegar, M. A., Kusche, J., Geremia-Nievinski, F., & Larson, K. M., 2022. Raspberry Pi Reflector (RPR): A low-cost water-level monitoring system based on GNSS interferometric reflectometry. *Water Resources Research*, 58(12).  
doi.org/10.1029/2021WR031713

Larson, K. M., & GNSS-IR community., 2024. What is a good GNSS reflections site? GNSS-IR Documentation. [gnssrefl.readthedocs.io/en/latest/pages/new\\_station.html#reflection-zones](https://gnssrefl.readthedocs.io/en/latest/pages/new_station.html#reflection-zones)

Larson, K. M., Ray, R. D., Nievinski, F. G., & Freymueller, J. T., 2013. The accidental tide gauge: a GPS reflection case study from Kachemak Bay, Alaska. *IEEE Geoscience and Remote Sensing Letters*, 10(5), 1200-1204.  
doi.org/10.1109/LGRS.2012.223607

Larson, K. M., & Williams, S. D. P., 2023. Water level measurements using reflected GNSS signals. *The International Hydrographic Review*, 29(2), 66–76.  
doi.org/10.58440/ihr-29-2-a30

Permanent Service for Mean Sea Level. (n.d.). An introduction to GNSS-IR. Permanent Service for Mean Sea Level. Retrieved from <https://psmsl.org/data/gnssir/introduction.php>

Roesler, C., & Larson, K. M., 2018. Software tools for GNSS interferometric reflectometry (GNSS-IR). *GPS Solutions*, 22(1), 1–10. doi.org/10.1007/s10291-018-0744-8

Siringan, F. P., & Maria, M. Y. Y., 2024. Sea level rise and coastal erosion in the Philippines: Impacts and adaptation Strategies for Coastal communities. In *Disaster risk reduction* (pp. 47–70). doi.org/10.1007/978-981-99-7804-5\_3

Stefal, 2025. RTKBase, Version 2.6.3. GitHub. [github.com/Stefal/rtkbase](https://github.com/Stefal/rtkbase) (6 June 2025).

Strandberg, J., Hobiger, T., & Haas, R., 2019. Real-time sea-level monitoring using Kalman filtering of GNSS-R data. *GPS Solutions*, 23(3). doi.org/10.1007/s10291-019-0851-1

Vidal, M., Jarrin, P., Rolland, L., Nocquet, J. M., Vergnolle, M., & Sakic, P., 2024. Cost-efficient multi-GNSS station with real-time transmission for geodynamics applications. *Remote Sensing*, 16(6), 991. doi.org/10.3390/rs16060991

Xu, T., Wang, N., He, Y., Li, Y., Meng, X., Gao, F., & Lopez-Baeza, E., 2024. GNSS Reflectometry-Based Ocean Altimetry: State of the Art and Future Trends. *Remote Sensing*, 16(10), 1754. doi.org/10.3390/rs16